ISSN 1028-334X, Doklady Earth Sciences, 2011, Vol. 438, Part 1, pp. 563–568. © Pleiades Publishing, Ltd., 2011.
Original Russian Text © A.V. Panin, 2011, published in Doklady Akademii Nauk, 2011, Vol. 438, No. 1, pp. 76–81.

GEOLOGY

New Data on the Late Holocene Seismicity of the Southwestern Edge of the Baikal Rift Zone

A. V. Panin

Presented by Academician N.S. Kasimov December 22, 2010

Received December 21, 2010

Abstract—Three strong earthquakes that occurred since the end of 8th century have been identified by archeoseismic data in the southwestern part of the Tere Khol' Depression. The dates for these events are the 9th, 12th, and first two-thirds of 19th century, and the average recurrence interval is 500 years. The relative seismic passivity of the Tere Khol' Depression at present may be related to the relatively recent discharge of stress in seismogenerating sources.

DOI: 10.1134/S1028334X11050060

The recurrence interval of strong earthquakes is one of the key parameters for seismic zoning of a territory [10]. In the paleoseismogeological sense, different parts of the Baikal Rift Zone are studied unequally, while particular ones are completely unstudied. The latter concerns the west branch of the southwestern closing of the Baikal Rift Zone that is represented by a series of three small graben depressions—the Belin, Buisingol, and Tere Khol' depressions. Data on seismic events within this area during the preinstrumental period are absent [8]. The closest paleoseismogeological studies were carried out in the area of the Akademik Obruchev Ridge, 100–150 km north of the Tere Khol' Depression, and they revealed Holocene paleoseismodislocations with calculated magnitudes of 6.5–7.4 [1]. The data of instrumental observations carried out since 1964 indicate a high seismic activity of the Buisingol Depression, where the earthquake with a magnitude of 6.5 was recorded in 1991 (energy class $K_p = 16.2$); additionally, three earthquakes of a lesser energy class ($K_p = 14.0–14.7$) were recorded in 1974, 1976, and 2005 [5]. During the past half-century, the Tere Khol' Depression was the least active: seismic events were rare here and only some of them reached $K_p = 12$. However, during geoarcheological studies in 2008, traces of several strong earthquakes that occurred in the last 1000–1200 years were found. In the present work, the results of diagnostics and dating for these paleoseismic events are given and then their recurrence interval is estimated.

The Tere Khol' Depression is a Late Cenozoic depression, overlain upon the Riphean structures of the Sangilen massif in the zone where it joins the Early Pale East Tannu-Ola block [3]. The rhombus-shaped outline of the depression suggests its evolution in accordance with the pull-apart basin or strike-slip rift scenario [9]. The Late Caledonian suture zone is represented by the recently activated northeast-striking Sangilen Fault that controls the northwestern side of the depression [11]. This side is a steep 400- to 500-m scarp with a series of dip-slip steps. Deformations of small valleys that cross it show the presence of young right-lateral motions with a summarized amplitude up to 200 m. Along the eastern side of the depression, a submeridional Arzhan Fault traverses, with the Buisingol and Belin depressions coinciding with it in the north [11].

In the southwestern corner of the Tere Khol' Depression, the shallow water Tere Khol' Lake is located; this lake is abundant with islands (Fig. 1). On one of the islands (50.615° N, 97.385° E), the Por-Bazhin complex is located; it is referred to the epoch of the Third Uighur Khaganate and is dated at about 750 A.D. [2]. The outer walls, trapezoidal in cross section and 8–9 m in height, form a rectangle of 160 × 220 m. Inside the walls, there is a system of internal courts with remains of dwelling rooms around the ruins of the central building (temple or palace). The walls of the courts have a residual height of 1.5–2 m. Both inner and outer walls are clayey, consist of rammed lake mud. The only brick construction is the foundation of the central building.

The island on which the architecture complex is located is composed of lake muds and alluvial sandy loam and is characterized by the presence of permafrost 15–20 m thick [6]. Additionally, there is a continuous thaw zone beneath the water area of the lake. The island therefore is a frozen lense among thawed rocks under strain, and this fact has a certain influence on how the island reacts to seismic effects.

Moscow State University, Moscow, 119991 Russia
e-mail: andrey-panin@rambler.ru

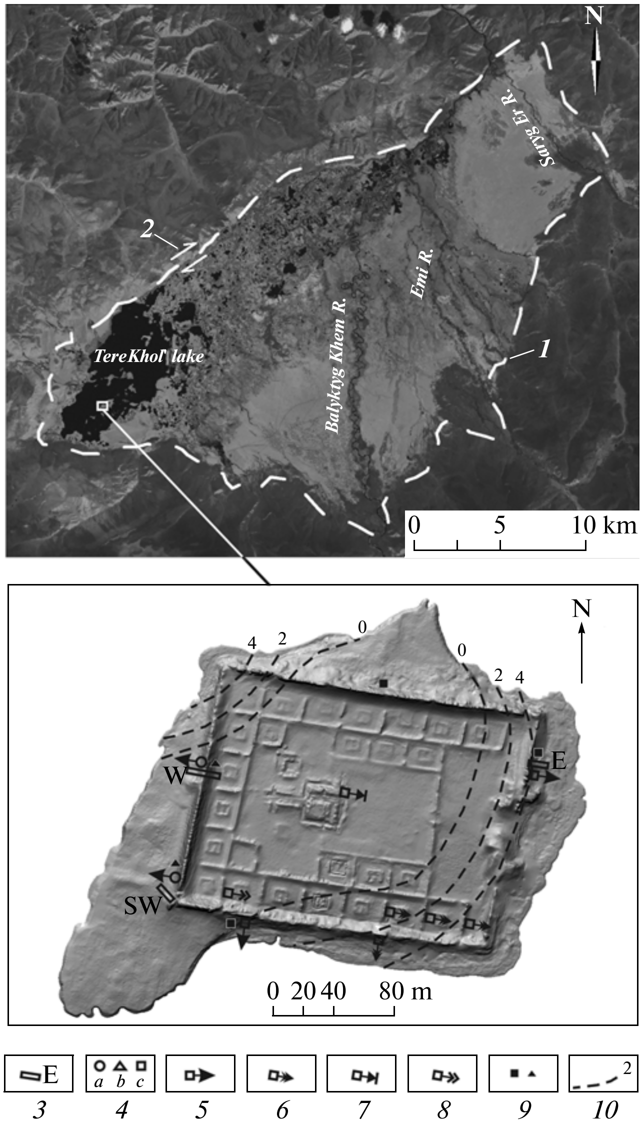

Fig. 1. The Tere Khol' Depression (Landsat-7 satellite image) and the Por-Bazhin Fortress (shaded relief image). The digital elevation model (DEM) was created by E.V. Selezneva (Faculty of Geography, Moscow State University) by the data of ground laser scanning given by the NPP Navgeokom. (*1*) Suture of the depression's bottom, limited by dip-slips; (*2*) directions of strike-slip displacements observed by deformations of small valleys; (*3*) position of the studied sections (E is eastern, W is western, SW is southwestern); (*4*) seismodeformations referring to various seismic events ((*a*) PSE-I, (*b*) PSE-II, (*c*) PSE-III); (*5–8*) directions of displacement: (*5*) collapsing of walls, (*6*) obliquing of walls, (*7*) falling out and obliquing of brickwork, (*8*) folding of ground; (*9*) local subsidences beneath walls; (*10*) isolines of subsidence depths, in meters.

Identification of paleoearthquakes was carried out by the seismogeological and archeoseismic data including the documenting of deformations in manmade constructions and of products of their destructions [7, 13]. The data for diagnostics and dating of paleoseismic events (PSEs) were obtained in trenches made across the talus piles at the base of the outer walls of the fortress. Absolute dating is carried out by the mass-spectrometric technique in the Radiocarbon Laboratory (University of Lund, Sweden). If not written another way, the age in text and figures is calendar; radiocarbon data are marked with "BP" (before present). Correspondence of the dates to calendar time is implemented in the OxCal 3.1 program [12] with the use of the calibrating curve IntCal'04 [14].

Dusty products of weathering in most of the talus piles contain three sod beds marking the relatively humid epochs (from bottom to top: Sod-1, Sod-2, and Sod-3). Three of the four outer walls (excluding the north one) were partially collapsed in various times via lateral flaking-off or collapse of a crest. Local depressions were found beneath all walls; they can be considered wall subsidences owing to compaction of the substrate during seismic quakes. The objects related to these subsidences and compaction of talus piles are systems of vertical cracks, associated to certain stratigraphic elements of geological sections depending on their age. Below we will consider the sections with available absolute dates in more detail (table).

The western trench contains traces of three PSEs (Fig. 2). The earliest of them is marked by collapse of the wall. Talus piles form a lense with maximal thickness of 0.9 m in the central part. In its roof, several exotic granite cobbles were found; most probably, they were on the crest of the wall at the moment of collapse.

The lense of fallen material is deformed resulting in later subsidence of the wall and adjacent part of the talus pile. Beneath the wall, subsidence is a little more than a meter. On aggregate, these signs (concave formation on the surface of the scree, appearance of a system of hollow cracks near the base of the scree, and microdip-slips directly beneath the wall owing to weight) indicate that subsidence occurred instantly and was caused by the next quake, namely, PSE-II.

The last earthquake (PSE-III) is traced by numerous subvertical cracks starting from the day surface. Microdip-slips with an amplitude of 5–7 cm are manifested in the form of scarps and stratigraphical displacements. Additional subsidence of the wall, if it took place, was of several centimeters. Judging by insufficient accumulation of weathering products upon the surface of scree after formation of seismogenic cracks, as well as by a good preservation of the microrelief, the age of this earthquake is not more than two–three centuries.

The southwestern trench exposes talus pile of the corner bastion. Traces of seismogenic failures here are analogous to those for the western trench (Fig. 2).

In the east trench, traces of the first two earthquakes were not found, but signs of the PSE-III are presented (Fig. 2). They are represented by a fallen mass lying upon the scree, by a local subsidence of up to 1.5 m, and by systems of crack and microdip-slips. The following sequence of deformations is recon-

Radiocarbon dates in sections made across the talus piles of the outer walls

No.	Trench	Dated material	Depth, stratigraphy	Lab. no. (LuS)	Age		Correlation with seismic events
					^{14}C, BP	calendar, A.D. (95%)	
1	E	plant detritus	59–67 cm, upper part of sod beneath the talus pile of the wall	7424	94 ± 25	1690–1920	before PSE-III
2	E	grass stem	89–90 cm, roof of sod beneath the talus pile of the wall	8137	107 ± 30	1690–1920	before PSE-III
3	E	grass stem	99–100 cm, of sod beneath the talus pile of the wall	8138	222 ± 30	1640–1960	before PSE-III
4	W	grass stem	70 cm, sod interbed (Sod-2)	8142	721 ± 35	1255–1295	after PSE-II
5	W	grass stem	105 cm, sod interbed (Sod-1)	8143	1135 ± 85	780–990	after PSE-I—before PSE-II
6	SW	grass stem	97 cm, sod beneath talus pile of the wall (Sod-1)	8141	1167 ± 30	780–940	after PSE-I—before PSE-II
7	W	skull of bird (order *Passeriformes*, family *Emberizidae*)	150 cm, the base of the talus pile of the wall	8144	1260 ± 50	670–810	before PSE-I
8	SW	grassy stem	185 cm, sod beneath the talus pile of the wall	8140	1425 ± 70	430–770	before PSE-I

structed. During the seismic quake occurrence, subsidence of the wall occurred and the near-wall zone of up to seven meters width was involved in it. Brittle deformations that accompanied concaving of the buried frozen surface formed systems of cracks and wedgelike subsidences that reach the day surface in some places and form microscarps (1–2 cm). Immediately after this, collapse of the wall occurred, and the fallen mass buried the surface of the talus pile. The fast burying of microscarps on the surface of the talus pile provided their preservation, because they would not have remained had they been exposed on the surface for a long time. The reconstruction made is applied to the south wall of the fortress, whose talus pile demonstrates an analogous statigraphic pattern with only one difference: the direction of fall is south in this case.

Among the other traces of seismic effects, the most notable are, first of all, subsidences in some parts of island; judging by the deformation of crests of outer walls, their amplitude reached 4–5 m (Fig. 1). These subsidences can be a cumulative effect of all three PSEs. Several features, which are most probably referred to the PSE-III, show the effect of horizontal shock waves from the east side (Fig. 1). For instance, in the southeastern part of the fortress, submeridionally oriented inner walls are located obliquely eastwards. In the eastern framing of the central construction, a typical feature is that some arrays of brickwork moved out eastwards. In some sublatitudinal sections of talus piles, folding of material in the eastern direction was found.

Estimation of the most probable occurrence time for the paleoseismic event is made on the basis of the probability density distribution of calendar age for the available radiocarbon dates (Fig. 3) and historical data.

The PSE-I time is limited on the bottom by the date of Por-Bazhin construction (mid-8th century A.D. [2]). In the western and southwestern trenches, products of the wall collapsing overlie the products of weathering in the base of wall (Fig. 2); i.e., the seismic event occurred a certain time later after the wall was constructed. The age of the fall is limited on bottom and on the top by the dates of 740 ± 70 and 885 ± 105 A.D., respectively, for the western trench, and by 600 ± 170 and 860 ± 80 A.D., respectively, for the southwestern trench. In the western trench, the material beneath the fallen material is stratigraphically closer to the moment of the event. It is a whole bird skull lying directly at the base of the fallen material. Any other bone remains were not found; hence, the bird, most probably, was not killed as a result of this material falling. However, a good preservation of the thin-walled skull, which was struck by falling material, and the absence of an interbed of weathering products between it and the scree signify that this skull was here not long before the seismic event. The best correspondence to the given facts is achieved if we consider that the PSE-I occurred during the 9th century A.D.

Subsidence of the western wall, referred to PSE-II, deforms Sod-1 (885 ± 105 A.D.), but it is already compensated by accumulative deposits at the level of Sod-2 (1275 ± 20 A.D.) (Fig. 2). Cracks that cut Sod-1 start closer to Sod-2; this allows us to suggest that the earthquake occurred closer to a later date. Proceeding from the dates of sod beds, the average sedimentation rate for the 55-cm layer of fine-grained material that divides Sod-1 and Sod-2 may be estimated at 0.16 ± 0.05 cm per 100 years. Hence, the upper level of cracks

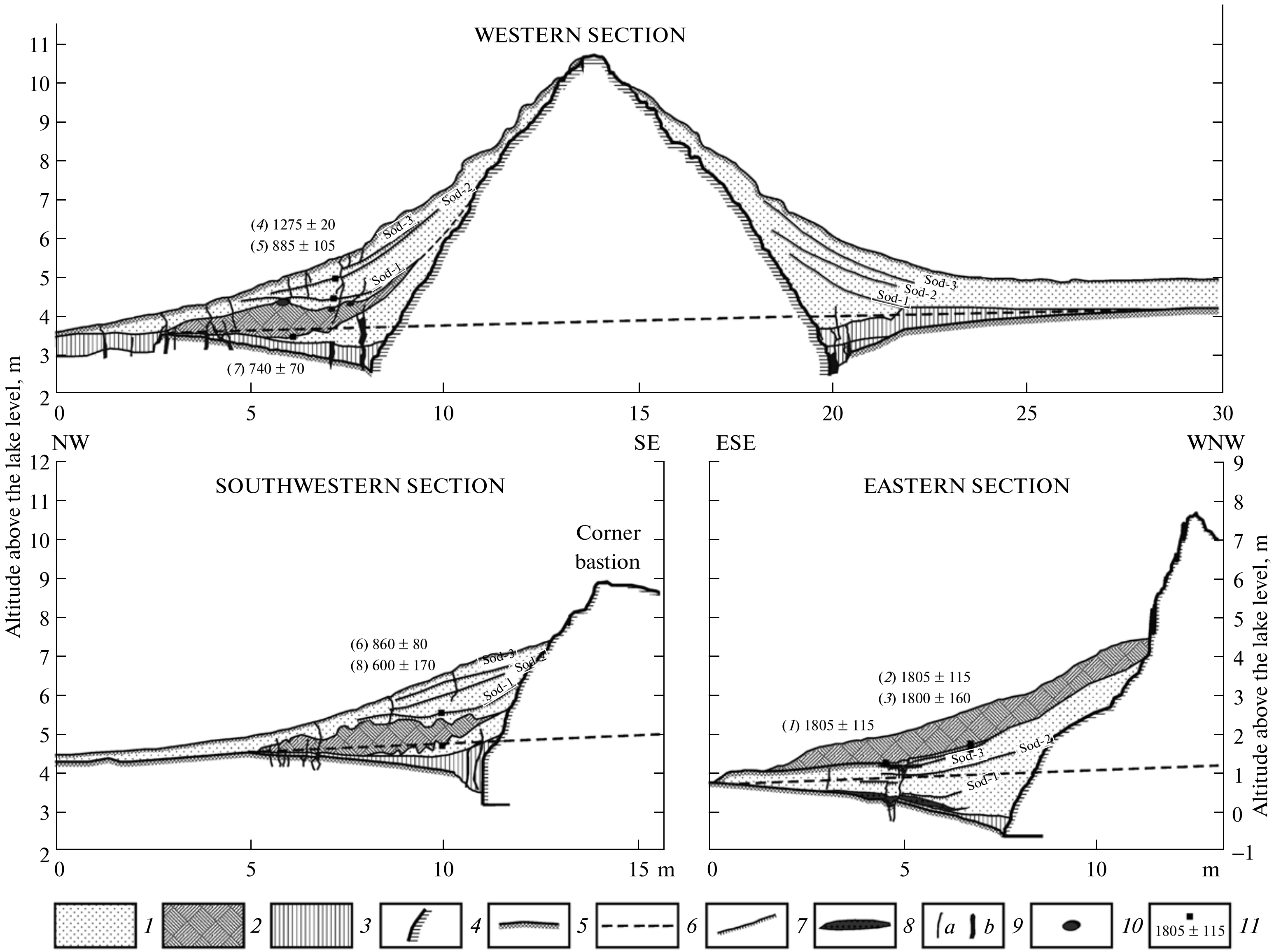

Fig. 2. Sections of talus piles at the base of the outer walls with recorded seismodeformations. (*1*) Fine-grained products of slow destruction of walls; (*2*) coarse-grained collapsed bodies; (*3*) rammed lake mud with wooden fragments; (*4*) surfaces of walls; (*5*) humus horizons of modern and buried soils; (*6*) initial position of soil roof (reconstruction); (*7*) buried sod; (*8*) coal-saturated lenses; (*9*) cracks ((*a*) closed, (*b*) opened); (*10*) granite cobbles; (*11*) position of samples and radiocarbon dates in calendar timescale (years A.D.), digits in brackets correspond to order numbers in the table.

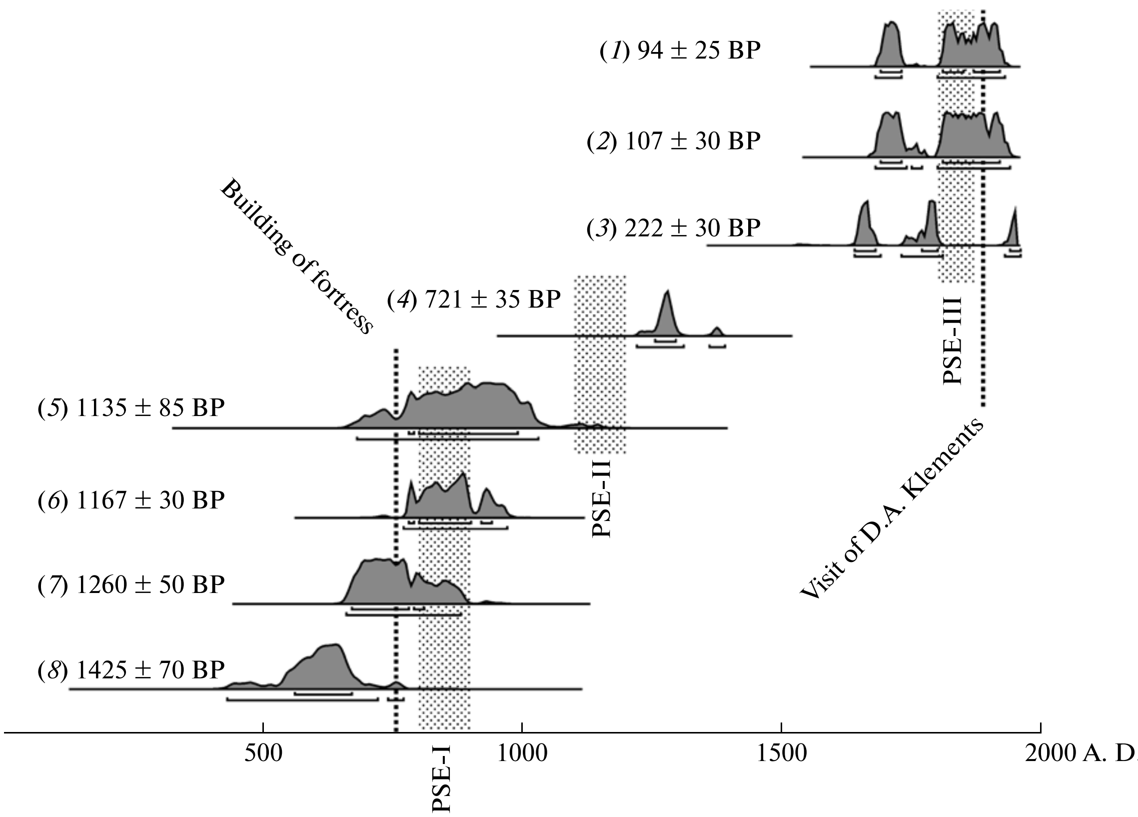

Fig. 3. Probability density distribution for radiocarbon dates and estimation of the most probable dates for paleoseismic events (PSE).

referring to the earthquake (20 cm below Sod-2) corresponds to the surface of the scree that existed 100–180 years before Sod-2 was formed. Thus, PSE-II occurred, most probably, during the 12th century A.D.

Dating of PSE-III is difficult because of its young age on the limit of the radiocarbon method's applicability. In the buried sod layers opened in the eastern trench, there are three dates that can be lower estimates for the age of the earthquake: 1800 ± 160, 1805 ± 115, and 1805 ± 115 A.D.; the first date is stratigraphically farther from the moment of the earthquake than the other two (Fig. 2). As is seen from Fig. 3, the calibration intervals of all these dates fall into two–three isolated sections that cover the period from the late 17th century to the mid-20th century on aggregate. The correlation of peaks for the lower and two upper dates indicates two intervals suitable for dating of the wall collapse: the boundary of 17th and 18th centuries and the 19th–mid-20th century. The former interval is less probable, because almost no products of weathering were accumulated on the surfaces of talus piles near both the eastern and southern walls. The upper limit of the earthquake's age can be assessed by the historical sources.

In 1891, D.A. Klements, participant of the Orkhon expedition of the Russian Geographic Society, was in Por-Bazhin. His report [4] contains descriptions of the state of the fortress walls that are very similar to the present state. In particular, he mentioned good preservation of the northern and western walls, in contrast to destructions of the southern and eastern walls. In addition, it was mentioned that the southern wall was located obliquely to the lakeside. Since the most significant destructions of the southern and eastern walls occurred during PSE-III, one can consider that the last earthquake had already occurred by the moment of Klements' vizit. Therefore, the most probable date for PSE-III is the first two-thirds of the 19th century.

The time gap between the first and second paleoearthquakes is about 300 years, while there was about 700 years between the second and third ones. Thus, the average recurrence interval of strong earthquakes can be estimated at 500 years. This conforms to the corresponding estimate for the southwestern region of the Baikal Rift Zone, made by statistical methods: 370 years for earthquakes with $K_p = 18$ [5]. The relative seismic passivity of the Tere Khol' Depression at present can be a consequence of the relatively recent discharge of stress in local seismogenerating sources.

ACKNOWLEDGMENTS

The author is grateful to I.A. Arzhantseva, M.A. Bronnikova, and V.A. Zav'yalov for their help in field studies and for fruitful discussions; and to E.V. Seleznyova for the digital elevation image. This work was supported by the Por-Bazhin Fortress Cultural Foundation and the Russian Foundation for Basic Research (project no. 09-05-00351).

REFERENCES

1. S. G. Arzhannikov, Geol. i Geofiz. **41** (11), 1499 (2000).
2. S. I. Vainshtein, Sov. Etnografiya, No. 6, 103 (1964).
3. E. P. Vasil'ev, V. G. Belichenko, and L. Z. Reznitskii, Dokl. Akad. Nauk **353** (6), 789 (1997).
4. D. A. Klements, *Archeological Diary on Travel to Middle Mongolia in 1891* (St. Petersburg, 1895) [in Russian].
5. A. V. Klyuchevskii, V. M. Dem'yanovich, and G. Bayar, Geol. i Geofiz. **46** (7), 746–762 (2005).
6. A. V. Koshurnikov, Yu. D. Zykov, A. V. Panin, et al., Inzhenernye Izyskaniya, No. 6, 28 (2008).
7. A. A. Nikonov, Voprosy inzhenernoi seismologii, issue 31, pp. 137–142.
8. *The New Catalogue of Strong Earthquakes within the Territory of Soviet Union since Ancient Times until 1975* (Nauka, Moscow, 1977) [in Russian].
9. O. P. Polyanskii and N. L. Dobretsov, Dokl. Akad. Nauk **380** (3), 368–373 (2001).
10. V. I. Ulomov, Vulkanologiya i Seismologiya, No. 4/5, 6 (1999).
11. G. A. Chernov, *Seismic Geology of the Eastern Part of the Altai-Sayan Mountain Region* (Nauka, Novosibirsk, 1978) [in Russian].
12. Ramsey C. Bronk, Oxford Radiocarbon Accelerator Unit, http://c14.arch.ox.ac.uk/oxcal.php.
13. F. Galadini, K.-G. Hinzen, and S. Stiros, J. Seismol. **10**, 395 (2006).
14. P. J. Reimer, M. G. L. Baillie, E. Bard, et al., Radiocarbon **46**, 1029 (2004).